



Available online at www.sciencedirect.com

ScienceDirect

**NUCLEAR
PHYSICS B**

Nuclear Physics B 886 (2014) 665–680

www.elsevier.com/locate/nuclphysb

Evidence for the decay $X(3872) \rightarrow \psi(2S)\gamma$

LHCb Collaboration

Received 2 April 2014; received in revised form 9 June 2014; accepted 11 June 2014

Available online 16 June 2014

Editor: Nuclear Physics B, Editorial Office

Abstract

Evidence for the decay mode $X(3872) \rightarrow \psi(2S)\gamma$ in $B^+ \rightarrow X(3872)K^+$ decays is found with a significance of 4.4 standard deviations. The analysis is based on a data sample of proton–proton collisions, corresponding to an integrated luminosity of 3 fb^{-1} , collected with the LHCb detector, at centre-of-mass energies of 7 and 8 TeV. The ratio of the branching fraction of the $X(3872) \rightarrow \psi(2S)\gamma$ decay to that of the $X(3872) \rightarrow J/\psi\gamma$ decay is measured to be

$$\frac{\mathcal{B}(X(3872) \rightarrow \psi(2S)\gamma)}{\mathcal{B}(X(3872) \rightarrow J/\psi\gamma)} = 2.46 \pm 0.64 \pm 0.29,$$

where the first uncertainty is statistical and the second is systematic. The measured value does not support a pure $D\bar{D}^*$ molecular interpretation of the $X(3872)$ state.

© 2014 The Authors. Published by Elsevier B.V. This is an open access article under the CC BY license (<http://creativecommons.org/licenses/by/3.0/>). Funded by SCOAP³.

1. Introduction

The $X(3872)$ state was discovered in 2003 by the Belle Collaboration [1]. Subsequently, it has been studied by several other experiments [2–6]. Several properties of the $X(3872)$ state have been determined, including the precise value of its mass [5,7] and the dipion mass spectrum in the decay $X(3872) \rightarrow J/\psi\pi^+\pi^-$ [1,6,8]. Recently, its quantum numbers were determined to be $J^{PC} = 1^{++}$ by combination of the measurements performed by the CDF [9] and the LHCb [10] Collaborations.

Despite a large amount of experimental information, the nature of $X(3872)$ state and other similar states is still uncertain [11,12]. In particular for the $X(3872)$ state, interpretation as a $D\bar{D}^*$ molecule [13], tetraquark [14], c_cg hybrid meson [15], vector glueball [16] or mixed state [17,18] are proposed. Radiative decays of the $X(3872)$ provide a valuable opportunity to understand its

<http://dx.doi.org/10.1016/j.nuclphysb.2014.06.011>

0550-3213/© 2014 The Authors. Published by Elsevier B.V. This is an open access article under the CC BY license (<http://creativecommons.org/licenses/by/3.0/>). Funded by SCOAP³.

nature. Studies of the decay modes $X(3872) \rightarrow J/\psi\gamma$ resulted in the determination of its C -parity [19,20]. Evidence for the $X(3872) \rightarrow \psi(2S)\gamma$ decay and the branching fraction ratio,

$$R_{\psi\gamma} \equiv \frac{\mathcal{B}(X(3872) \rightarrow \psi(2S)\gamma)}{\mathcal{B}(X(3872) \rightarrow J/\psi\gamma)} = 3.4 \pm 1.4,$$

were reported by the BaBar Collaboration [21]. In contrast, no significant signal was found for the $X(3872) \rightarrow \psi(2S)\gamma$ decay by the Belle Collaboration, therefore only an upper limit for $R_{\psi\gamma} < 2.1$ (at 90% confidence level) was reported [20]. The ratio $R_{\psi\gamma}$ is predicted to be in the range $(3\text{--}4) \times 10^{-3}$ for a $D\bar{D}^*$ molecule [22–24], 1.2–15 for a pure charmonium state [25–32] and 0.5–5 for a molecule-charmonium mixture [29,33].

In this paper, evidence for the decay $X(3872) \rightarrow \psi(2S)\gamma$ and a measurement of the ratio $R_{\psi\gamma}$ using $B^+ \rightarrow X(3872)K^+$ decays are presented.¹ The analysis is based on a data sample of proton–proton (pp) collisions, corresponding to an integrated luminosity of 1 fb^{-1} at a centre-of-mass energy of 7 TeV and 2 fb^{-1} at 8 TeV, collected with the LHCb detector.

2. Detector and software

The LHCb detector [34] is a single-arm forward spectrometer covering the pseudorapidity range $2 < \eta < 5$, designed for the study of particles containing b or c quarks. The detector includes a high-precision tracking system consisting of a silicon-strip vertex detector surrounding the pp interaction region, a large-area silicon-strip detector located upstream of a dipole magnet with a bending power of about 4 Tm, and three stations of silicon-strip detectors and straw drift tubes placed downstream. The combined tracking system provides a momentum measurement with relative uncertainty that varies from 0.4% at $5 \text{ GeV}/c$ to 0.6% at $100 \text{ GeV}/c$, and impact parameter resolution of $20 \mu\text{m}$ for tracks with high transverse momentum. Charged hadrons are identified using two ring-imaging Cherenkov detectors [35]. The calorimeter system consists of a scintillating pad detector (SPD) and a pre-shower system (PS), followed by electromagnetic (ECAL) and hadron calorimeters. The SPD and PS are designed to distinguish between signals from photons and electrons. Muons are identified by a system composed of alternating layers of iron and multiwire proportional chambers [36].

The trigger [37] consists of a hardware stage, based on information from the calorimeter and muon systems, followed by a software stage where a full event reconstruction is applied. This analysis uses events collected by triggers that select the $\mu^+\mu^-$ pair from J/ψ and $\psi(2S)$ decays with high efficiency. At the hardware stage either one or two muon candidates are required to trigger the event. For single muon triggers, the transverse momentum of the muon candidate, p_T , is required to be greater than $1.48 \text{ GeV}/c$. For dimuon candidates, the product of the p_T of the muon candidates is required to satisfy $\sqrt{p_T(\mu^+) \times p_T(\mu^-)} > 1.3 \text{ GeV}/c$. At the subsequent software trigger stage, two muons are selected with an invariant mass larger than $2.5 \text{ GeV}/c^2$ and consistent with originating from a common vertex. The common vertex is required to be significantly displaced from the pp collision vertices by requiring the decay length significance to be greater than 3.

The analysis technique reported below has been validated using simulated events. The pp collisions are generated using PYTHIA [38] with a specific LHCb configuration described in Ref. [39]. Decays of hadronic particles are described by EVTGEN [40] in which final state radiation is generated using PHOTOS package [41]. The interaction of the generated particles with

¹ The inclusion of charged conjugate processes is implied throughout.

the detector and its response are implemented using the GEANT4 toolkit [42,43] as described in Ref. [44].

3. Event selection

Candidate $B^+ \rightarrow X(3872)K^+$ decays, followed by $X(3872) \rightarrow \psi\gamma$, where ψ denotes a J/ψ or $\psi(2S)$ meson, are reconstructed using the $\psi \rightarrow \mu^+\mu^-$ channel. The $\psi(2S) \rightarrow J/\psi\pi^+\pi^-$ decay mode is not used due to low reconstruction efficiency. Most selection criteria are common for the two channels, except where directly related to the photon kinematics, due to the difference in the energy release in these two channels. The selection criteria follow those used in Refs. [45–47].

The track quality of reconstructed charged particles is ensured by requiring that the χ^2 per degree of freedom, χ^2/ndf , is less than 3. Well-identified muons are selected by requiring that the difference in the logarithms of the muon hypothesis likelihood with respect to the pion hypothesis likelihood, $\Delta \log \mathcal{L}_{\mu/\pi}$ [48], is larger than zero. To select kaons, the corresponding difference in the logarithms of likelihoods of the kaon and pion hypotheses [35] is required to satisfy $\Delta \log \mathcal{L}_{K/\pi} > 0$.

To ensure that the muons and kaons do not originate from a pp interaction vertex, the impact parameter χ^2 , defined as the difference between the χ^2 of a given PV formed with and without the considered track, is required to be When more than one PV is reconstructed, the smallest value of χ^2_{IP} is chosen.

Pairs of oppositely charged tracks identified as muons, each having $p_T > 0.55 \text{ GeV}/c$, are combined to form $\psi \rightarrow \mu^+\mu^-$ candidates. The fit of the common two-prong vertex is required to satisfy $\chi^2/\text{ndf} < 20$. The vertex is required to be well separated from the reconstructed PV by selecting candidates with decay length significance greater than 3. The invariant mass of the dimuon combination is required to be between 3.020 and $3.135 \text{ GeV}/c^2$ for the J/ψ candidates and between 3.597 and $3.730 \text{ GeV}/c^2$ for the $\psi(2S)$ candidates. The selected ψ candidates are required to match the dimuon candidates used to trigger the event.

Photons are reconstructed using the electromagnetic calorimeter and identified using a likelihood-based estimator, constructed from variables that rely on calorimeter and tracking information [49]. Candidate photon clusters must not be matched to the trajectory of a track extrapolated from the tracking system to the cluster position in the calorimeter. Further photon quality refinement is done using information from the PS and SPD detectors. The photon transverse momentum is required to be greater than $1 \text{ GeV}/c$ or $0.6 \text{ GeV}/c$ for the J/ψ or $\psi(2S)$ in the final state, respectively. To suppress the large combinatorial background from $\pi^0 \rightarrow \gamma\gamma$ decays, a pion veto is applied [46]. The photons that, when combined with another photon, form a $\pi^0 \rightarrow \gamma\gamma$ candidate with invariant mass within $25 \text{ MeV}/c^2$ of the π^0 mass, corresponding to ± 3 times the mass resolution [46,50], are not used in the reconstruction.

To form $X(3872)$ candidates, the selected ψ candidates are combined with a reconstructed photon. To be considered as a $X(3872)$ candidate, the $J/\psi\gamma$ or $\psi(2S)\gamma$ combination must have an invariant mass in the range 3.7 – $4.1 \text{ GeV}/c^2$ or 3.75 – $4.05 \text{ GeV}/c^2$, respectively, to account for the different available phase space.

The $X(3872)$ candidates are combined with selected kaons to create B^+ meson candidates. The kaons are required to have transverse momentum larger than $0.8 \text{ GeV}/c$. The quality of the B^+ vertex is ensured by requiring the χ^2/ndf of the vertex fit to be less than $25/3$. In addition, the decay time of the B^+ is required to be larger than $150 \mu\text{m}/c$ to reduce the large combinatorial background from particles produced at the PV.

To improve the invariant mass resolution of the $X(3872)$ candidate, a kinematic fit [51] is performed. In this fit, the invariant mass of the ψ candidate is constrained to its nominal value [52], the decay products of the B^+ candidate are required to originate from a common vertex, and the momentum vector of the B^+ candidate is required to point back to the PV. The χ^2/ndf for this fit is required to be less than 5. To improve the resolution on the B^+ candidate invariant mass, and reduce its correlation with the reconstructed $X(3872)$ candidate mass, the B^+ mass is determined from a similar kinematic fit with an additional constraint applied to the mass of the $X(3872)$ resonance [52]. The B^+ candidates are required to have invariant mass in the range $5.0\text{--}5.5\text{ GeV}/c^2$. To reject possible contributions from $B^+ \rightarrow \psi K^+$ decays with an additional random soft photon, the invariant mass of the ψK^+ combination is required to be outside a $\pm 40\text{ MeV}/c^2$ mass window around the known B^+ mass [52].

4. Signal yields

To determine the signal yield of the $B^+ \rightarrow X(3872)K^+$ decays followed by $X(3872) \rightarrow \psi\gamma$, an unbinned extended maximum likelihood two-dimensional fit in $\psi\gamma K^+$ and $\psi\gamma$ invariant masses is performed. The probability density function used in the fit consists of three components to describe the mass spectrum: signal, background from other B decays that peaks in the $\psi\gamma K^+$ and $\psi\gamma$ invariant mass distributions (henceforth called “peaking background”) and pure combinatorial background.

The signal component is modelled as a product of a Gaussian function in the $\psi\gamma K^+$ invariant mass and a Crystal Ball function [53] in the $\psi\gamma$ invariant mass. The mass resolution and tail parameters of the Crystal Ball function are fixed to those determined from simulated signal events.

The peaking background is studied using simulation. The sources of the peaking background are different in the J/ψ and $\psi(2S)$ channels due to differences in the photon spectra and in the photon selection requirements in these two channels. The main source of the peaking background in the J/ψ channel is the partially reconstructed $B^+ \rightarrow J/\psi K^{*+}$ decays followed by $K^{*+} \rightarrow K^+\pi^0$ where one photon from the π^0 decay is not detected. In the $\psi(2S)$ channel the peaking background arises from partially reconstructed $B \rightarrow \psi(2S)K^+Y$ decays combined with a random photon, where B denotes a b hadron and Y denotes additional particles of the B decay, that escape detection. These background contributions are modelled in the fit using non-parametric kernel probability density functions [54], obtained from simulation of B decays to final states containing a J/ψ or $\psi(2S)$ meson.

Pure combinatorial background is modelled as the product of an exponential function of the $\psi\gamma K^+$ invariant mass and a second-order polynomial function of the $J/\psi\gamma$ invariant mass or a third-order polynomial function of the $\psi(2S)\gamma$ invariant mass. For the latter case, the polynomial function is constrained to account for the small available phase space, allowing only two polynomial degrees of freedom to vary in the fit.

The significance of the observed signal in the $\psi(2S)$ channel is determined by simulating a large number of background-only experiments, taking into account all uncertainties in the shape of the background distribution. The probability for the background to fluctuate to at least the number of observed events is found to be 1.2×10^{-5} , corresponding to a significance of 4.4 standard deviations for the $B^+ \rightarrow X(3872)K^+$ decay followed by $X(3872) \rightarrow \psi(2S)\gamma$.

The fit results for the position of the B^+ and $X(3872)$ mass peaks, m_{B^+} and $m_{X(3872)}$, respectively, and the signal yields N_ψ are listed in Table 1. Projections of the fit on $\psi\gamma K^+$ and $\psi\gamma$ invariant masses are shown in Figs. 1 and 2 for the J/ψ and $\psi(2S)$ channels, respectively.

Table 1

Parameters of the signal functions of the fits to the two-dimensional mass distributions of the $B^+ \rightarrow X(3872)K^+$ decays followed by $X(3872) \rightarrow \psi\gamma$. Uncertainties are statistical only.

Parameter	Decay mode	
	$X(3872) \rightarrow J/\psi\gamma$	$X(3872) \rightarrow \psi(2S)\gamma$
m_{B^+} [MeV/ c^2]	5277.7 ± 0.8	5281.9 ± 2.4
$m_{X(3872)}$ [MeV/ c^2]	3873.4 ± 3.4	3869.5 ± 3.4
N_ψ	591 ± 48	36.4 ± 9.0

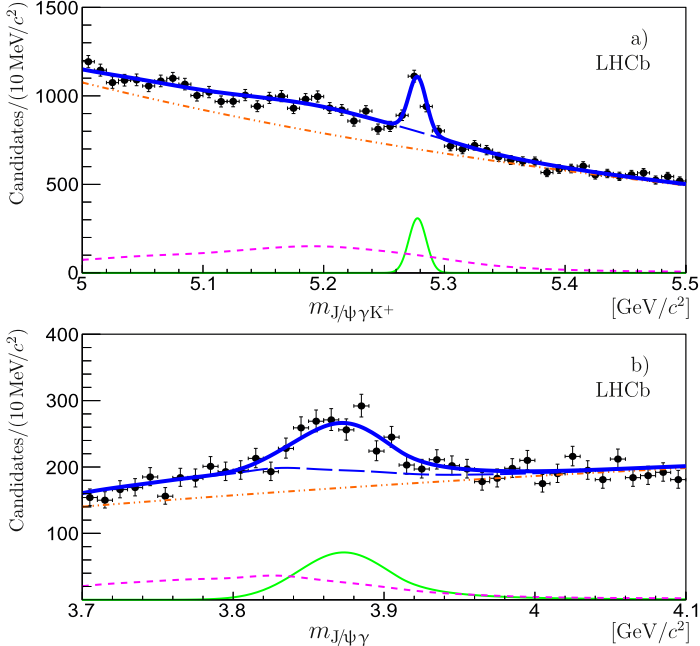


Fig. 1. a) Distribution of the $J/\psi\gamma K^+$ invariant mass with fit projection overlaid, restricted to those candidates with $J/\psi\gamma$ invariant mass within $\pm 3\sigma$ from the $X(3872)$ peak position. b) Distribution of the $J/\psi\gamma$ invariant mass with fit projection overlaid, restricted to those candidates with $J/\psi\gamma K^+$ invariant mass within $\pm 3\sigma$ from the B^+ peak position. The total fit (thick solid blue) together with the signal (thin solid green) and background components (dash-dotted orange for the pure combinatorial, dashed magenta for the peaking component and long dashed blue for their sum) are shown. (For interpretation of the references to color in this figure legend, the reader is referred to the web version of this article.)

5. Efficiencies and systematic uncertainties

The ratio of the $X(3872) \rightarrow \psi(2S)\gamma$ and $X(3872) \rightarrow J/\psi\gamma$ branching fractions is calculated using the formula

$$R_{\psi\gamma} = \frac{N_{\psi(2S)}}{N_{J/\psi}} \times \frac{\varepsilon_{J/\psi}}{\varepsilon_{\psi(2S)}} \times \frac{\mathcal{B}(J/\psi \rightarrow \mu^+\mu^-)}{\mathcal{B}(\psi(2S) \rightarrow \mu^+\mu^-)}, \quad (1)$$

where $N_{J/\psi}$ and $N_{\psi(2S)}$ are the measured yields listed in Table 1, and $\varepsilon_{J/\psi}$ and $\varepsilon_{\psi(2S)}$ are the total efficiencies. For the ratio of the $\psi \rightarrow \mu^+\mu^-$ branching fractions, lepton universality is assumed and a ratio of dielectron branching fractions equal to 7.60 ± 0.18 [52] is used. The uncertainty is treated as a systematic uncertainty.

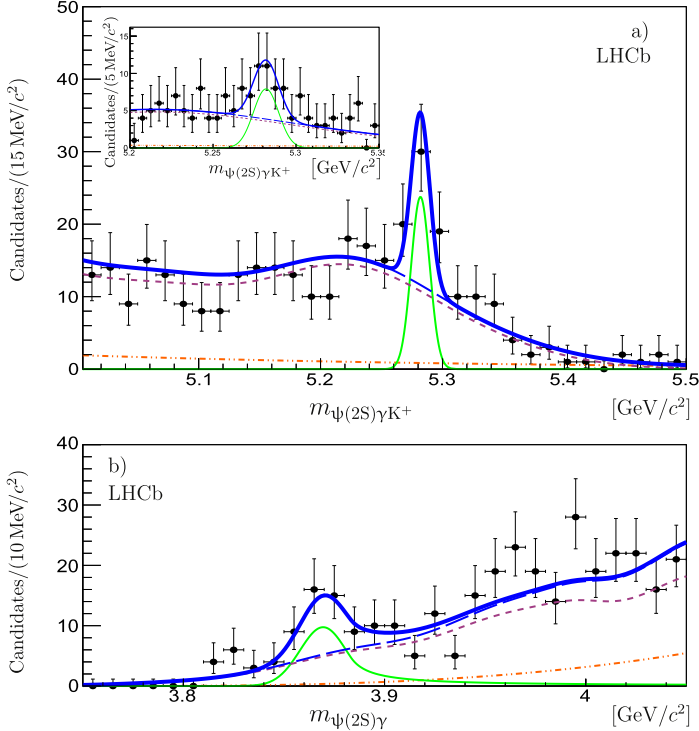


Fig. 2. a) Distribution of the $\psi(2S)\gamma K^+$ invariant mass with fit projection overlaid, restricted to those candidates with $\psi(2S)\gamma$ invariant mass within $\pm 3\sigma$ from the $X(3872)$ peak position (the inset shows a zoom of the $\psi(2S)\gamma K^+$ mass region). b) Distribution of the $\psi(2S)\gamma$ invariant mass with fit projection overlaid, restricted to those candidates with $\psi(2S)\gamma K^+$ invariant mass within $\pm 3\sigma$ from the B^+ peak position. The total fit (thick solid blue) together with the signal (thin solid green) and background components (dash-dotted orange for the pure combinatorial, dashed magenta for the peaking component and long dashed blue for their sum) are shown. (For interpretation of the references to color in this figure legend, the reader is referred to the web version of this article.)

The total efficiency is the product of the geometrical acceptance, the detection, reconstruction, selection and trigger efficiencies. The efficiencies are estimated using simulated events that have been corrected to reproduce the observed kinematics of B^+ mesons using the high-yield decay $B^+ \rightarrow \chi_{c1} K^+$ with $\chi_{c1} \rightarrow J/\psi \gamma$, which has a topology and kinematics similar to those of the decays under study. The ratio of the efficiencies is found to be $\varepsilon_{J/\psi}/\varepsilon_{\psi(2S)} = 5.25 \pm 0.04$, where the uncertainty is due to finite size of the simulated samples. The ratio of efficiencies is different from unity mainly because of the different photon spectra in the decays with J/ψ and $\psi(2S)$ in the final state.

Most sources of systematic uncertainty cancel in the ratio, in particular those related to the kaon, muon and ψ reconstruction and identification. The remaining systematic uncertainties are summarized in Table 2 and discussed in turn in the following.

Systematic uncertainties related to the signal yield determination are considered in four categories: signal, peaking background, combinatorial background and intervals used in the fit. For each category individual uncertainties are estimated using a number of alternative fit models. The maximum deviations from the baseline values of the yields are taken as individual systematic uncertainties, which are then added in quadrature. The systematic uncertainties on the event yields

Table 2
Relative systematic uncertainties on the ratio of branching fractions ($R_{\psi\gamma}$).

Source	Uncertainty [%]
X(3872) → J/ψγ yield determination	6
X(3872) → ψ(2S)γ yield determination	7
Photon reconstruction	6
B ⁺ kinematics	3
Selection criteria	2
Trigger	1
$\mathcal{B}(J/\psi \rightarrow e^+e^-)/\mathcal{B}(\psi(2S) \rightarrow e^+e^-)$	2
Simulation sample size	1
Sum in quadrature	12

are dominated by uncertainties in the description of backgrounds and are 6% and 7% in the J/ψ and ψ(2S) channels, respectively.

Another important source of systematic uncertainty arises from the potential disagreement between data and simulation in the estimation of efficiencies. This includes the photon reconstruction efficiency, the imperfect knowledge of B⁺ kinematics and the description of the selection criteria efficiencies. The photon reconstruction efficiency is studied using a large sample of B⁺ → J/ψK^{*+} decays, followed by K^{*+} → K⁺π⁰ and π⁰ → γγ decays. The relative yields of B⁺ → J/ψK^{*+} and B⁺ → J/ψK⁺ decays are compared in data and simulation. For photons with transverse momentum greater than 0.6 GeV/c, the agreement between data and simulation is within 6%, which is assigned as the systematic uncertainty due to the photon reconstruction.

The systematic uncertainty related to the knowledge of the B⁺ production properties is estimated by comparing the ratio of efficiencies determined without making corrections to the B⁺ transverse momentum and rapidity spectra to the default ratio of efficiencies determined after the corrections. The relative difference between the two methods is found to be 3% and is conservatively assigned as the systematic uncertainty from this source.

To study the uncertainty due to selection criteria, the high-yield decay B⁺ → χ_{c1}K⁺, followed by χ_{c1} → J/ψγ, which has a similar topology to the decays studied in this analysis, is used. The selection criteria for the photon and kaon transverse momentum, the π⁰ → γγ veto and the χ²/ndf of the kinematic fit are studied. The selection criteria are varied in ranges corresponding to as much as a 30% change in the signal yields and the ratios of the selection and reconstruction efficiencies are compared between data and simulation. The largest difference of 2% is assigned as the corresponding systematic uncertainty.

The systematic uncertainty related to the trigger efficiency is obtained by comparing the trigger efficiency ratios in data and simulation for the high yield decay modes B⁺ → J/ψK⁺ and B⁺ → ψ(2S)K⁺, which have similar kinematics and the same trigger requirements as the channels under study in this analysis [55]. An agreement within 1% is found, which is assigned as the corresponding systematic uncertainty.

6. Results and summary

Using a sample of pp collisions at centre-of-mass energies of 7 and 8 TeV, corresponding to an integrated luminosity of 3 fb⁻¹, evidence for the decay X(3872) → ψ(2S)γ in B⁺ → X(3872)K⁺ decays is found with a significance of 4.4 standard deviations. Its branching fraction, normalized to that of the X(3872) → J/ψγ decay mode is measured to be

$$R_{\psi\gamma} = \frac{\mathcal{B}(X(3872) \rightarrow \psi(2S)\gamma)}{\mathcal{B}(X(3872) \rightarrow J/\psi\gamma)} = 2.46 \pm 0.64 \pm 0.29,$$

where the first uncertainty is statistical and the second is systematic. This result is compatible with, but more precise than, previous measurements [20,21]. The measured value of $R_{\psi\gamma}$ does not support a pure $D\bar{D}^*$ molecular interpretation [22–24] of the X(3872) state, whereas it agrees with expectations for a pure charmonium interpretation of the X(3872) state [25–32] and a molecular-charmonium mixture interpretations [29,33].

Acknowledgements

We express our gratitude to our colleagues in the CERN accelerator departments for the excellent performance of the LHC. We thank the technical and administrative staff at the LHCb institutes. We acknowledge support from CERN and from the national agencies: CAPES, CNPq, FAPERJ and FINEP (Brazil); NSFC (China); CNRS/IN2P3 and Region Auvergne (France); BMBF, DFG, HGF and MPG (Germany); SFI (Ireland); INFN (Italy); FOM and NWO (The Netherlands); SCSR (Poland); MEN/IFA (Romania); MinES, Rosatom, RFBR and NRC “Kurchatov Institute” (Russia); MinECo, XuntaGal and GENCAT (Spain); SNSF and SER (Switzerland); NASU (Ukraine); STFC and the Royal Society (United Kingdom); NSF (USA). We also acknowledge the support received from EPLANET, Marie Curie Actions and the ERC under FP7. The Tier1 computing centres are supported by IN2P3 (France), KIT and BMBF (Germany), INFN (Italy), NWO and SURF (The Netherlands), PIC (Spain), GridPP (United Kingdom). We are indebted to the communities behind the multiple open source software packages on which we depend. We are also thankful for the computing resources and the access to software R&D tools provided by Yandex LLC (Russia).

References

- [1] Belle Collaboration, S.-K. Choi, et al., Observation of a narrow charmonium-like state in exclusive $B^+ \rightarrow K^+\pi^+\pi^-J/\psi$ decays, *Phys. Rev. Lett.* 91 (2003) 262001, arXiv:hep-ex/0309032.
- [2] CDF Collaboration, D. Acosta, et al., Observation of the narrow state $X(3872) \rightarrow J/\psi\pi^+\pi^-$ in $\bar{p}p$ collisions at $\sqrt{s} = 1.96$ TeV, *Phys. Rev. Lett.* 93 (2004) 072001, arXiv:hep-ex/0312021.
- [3] D0 Collaboration, V.M. Abazov, et al., Observation and properties of the X(3872) decaying to $J/\psi\pi^+\pi^-$ in $p\bar{p}$ collisions at $\sqrt{s} = 1.96$ TeV, *Phys. Rev. Lett.* 93 (2004) 162002, arXiv:hep-ex/0405004.
- [4] BaBar Collaboration, B. Aubert, et al., Study of the $B^- \rightarrow J/\psi K^-\pi^+\pi^-$ decay and measurement of the $B^- \rightarrow X(3872)K^-$ branching fraction, *Phys. Rev. D* 71 (2005) 071103, arXiv:hep-ex/0406022.
- [5] LHCb Collaboration, R. Aaij, et al., Observation of X(3872) production in pp collisions at $\sqrt{s} = 7$ TeV, *Eur. Phys. J. C* 72 (2012) 1972, arXiv:1112.5310.
- [6] CMS Collaboration, S. Chatrchyan, et al., Measurement of the X(3872) production cross section via decays to $J/\psi\pi^+\pi^-$ in pp collisions at $\sqrt{s} = 7$ TeV, *J. High Energy Phys.* 04 (2013) 154, arXiv:1302.3968.
- [7] CDF Collaboration, T. Aaltonen, et al., Precision measurement of the X(3872) mass in $J/\psi\pi^+\pi^-$ decays, *Phys. Rev. Lett.* 103 (2009) 152001, arXiv:0906.5218.
- [8] CDF Collaboration, A. Abulencia, et al., Measurement of the dipion mass spectrum in $X(3872) \rightarrow J/\psi\pi^+\pi^-$ decays, *Phys. Rev. Lett.* 96 (2006) 102002, arXiv:hep-ex/0512074.
- [9] CDF Collaboration, A. Abulencia, et al., Analysis of the quantum numbers J^{PC} of the X(3872) particle, *Phys. Rev. Lett.* 98 (2007) 132002, arXiv:hep-ex/0612053.
- [10] LHCb Collaboration, R. Aaij, et al., Determination of the X(3872) quantum numbers, *Phys. Rev. Lett.* 110 (2013) 222001, arXiv:1302.6269.
- [11] S. Godfrey, S.L. Olsen, The exotic XYZ charmonium-like mesons, *Annu. Rev. Nucl. Part. Sci.* 58 (2008) 51, arXiv:0801.3867.
- [12] S.-L. Zhu, et al., XYZ states, *PoS Hadron 2013* (2013) 005, arXiv:1311.3763.
- [13] E.S. Swanson, Diagnostic decays of the X(3872), *Phys. Lett. B* 598 (2004) 197, arXiv:hep-ph/0406080.

- [14] L. Maiani, F. Piccinini, A.D. Polosa, V. Riquer, Diquark–antidiquark states with hidden or open charm and the nature of X(3872), Phys. Rev. D 71 (2005) 014028, arXiv:hep-ph/0412098.
- [15] B.A. Li, Is X(3872) a possible candidate as a hybrid meson?, Phys. Lett. B 605 (2005) 306, arXiv:hep-ph/0410264.
- [16] K.K. Seth, An alternative interpretation of X(3872), Phys. Lett. B 612 (2005) 1, arXiv:hep-ph/0411122.
- [17] R.D. Matheus, F.S. Navarra, M. Nielsen, C.M. Zanetti, QCD sum rules for the X(3872) as a mixed molecule-charmonium state, Phys. Rev. D 80 (2009) 056002, arXiv:0907.2683.
- [18] W. Chen, et al., QCD sum-rule interpretation of X(3872) with $J^{PC} = 1^{++}$ mixtures of hybrid charmonium and $\bar{D}\bar{D}^*$ molecular currents, Phys. Rev. D 88 (2013) 045027, arXiv:1305.0244.
- [19] BaBar Collaboration, B. Aubert, et al., Search for $B^+ \rightarrow X(3872)K^+$, $X(3872) \rightarrow J/\psi\gamma$, Phys. Rev. D 74 (2006) 071101, arXiv:hep-ex/0607050.
- [20] Belle Collaboration, V. Bhardwaj, et al., Observation of $X(3872) \rightarrow J/\psi\gamma$ and search for $X(3872) \rightarrow \psi'\gamma$ in B decays, Phys. Rev. Lett. 107 (2011) 091803, arXiv:1105.0177.
- [21] BaBar Collaboration, B. Aubert, et al., Evidence for $X(3872) \rightarrow \psi(2S)\gamma$ in $B^\pm \rightarrow X(3872)K^\pm$ decays, and a study of $B \rightarrow c\bar{c}\gamma K$, Phys. Rev. Lett. 102 (2009) 132001, arXiv:0809.0042.
- [22] E.S. Swanson, Molecular interpretation of the X(3872), Phys. Lett. B 588 (2004) 189, arXiv:hep-ph/0410284.
- [23] Y. Dong, A. Faessler, T. Gutsche, V.E. Lyubovitskij, $J/\psi\gamma$ and $\psi(2S)\gamma$ decay modes of the X(3872), J. Phys. G 38 (2011) 015001, arXiv:0909.0380.
- [24] J. Ferretti, G. Galata, Quark structure of the X(3872) and $\chi_b(3P)$ resonances, arXiv:1401.4431.
- [25] T. Barnes, S. Godfrey, E.S. Swanson, Higher charmonia, Phys. Rev. D 72 (2005) 054026, arXiv:hep-ph/0505002.
- [26] T. Barnes, S. Godfrey, Charmonium options for the X(3872), Phys. Rev. D 69 (2004) 054008, arXiv:hep-ph/0311162.
- [27] B.-Q. Li, K.-T. Chao, Higher charmonia and X, Y, Z states with screened potential, Phys. Rev. D 79 (2009) 094004, arXiv:0903.5506.
- [28] T.A. Lahde, Exchange current operators and electromagnetic dipole transitions in heavy quarkonia, Nucl. Phys. A 714 (2003) 183, arXiv:hep-ph/0208110.
- [29] A.M. Badalini, V.D. Orlovsky, Y.A. Simonov, B.L.G. Bakker, The ratio of decay widths of X(3872) to $\psi'\gamma$ and $J/\psi\gamma$ as a test of the X(3872) dynamical structure, Phys. Rev. D 85 (2012) 114002, arXiv:1202.4882 [hep-ph].
- [30] T. Mehen, R. Springer, Radiative decays $X(3872) \rightarrow \psi(2S) + \gamma$ and $\psi(4040) \rightarrow X(3872) + \gamma$ in effective field theory, Phys. Rev. D 83 (2011) 094009, arXiv:1101.5175.
- [31] T.M. Wang, G.L. Wang, Radiative E1 decays of X(3872), Phys. Lett. B 697 (2011) 3, arXiv:1006.3363.
- [32] F. De Fazio, Radiative transitions of heavy quarkonium states, Phys. Rev. D 79 (2009) 054015;
F. De Fazio, Erratum: Radiative transitions of heavy quarkonium states [Phys. Rev. D 79, 054015 (2009)], Phys. Rev. D 83 (2011) 099901.
- [33] E.J. Eichten, K. Lane, C. Quigg, New states above charm threshold, Phys. Rev. D 73 (2006) 014014, arXiv:hep-ph/0511179.
- [34] LHCb Collaboration, A.A. Alves Jr., et al., The LHCb detector at the LHC, J. Instrum. 3 (2008) S08005.
- [35] M. Adinolfi, et al., Performance of the LHCb RICH detector at the LHC, Eur. Phys. J. C 73 (2013) 2431, arXiv:1211.6759.
- [36] A.A. Alves Jr., et al., Performance of the LHCb muon system, J. Instrum. 8 (2013) P02022, arXiv:1211.1346.
- [37] R. Aaij, et al., The LHCb trigger and its performance in 2011, J. Instrum. 8 (2013) P04022, arXiv:1211.3055.
- [38] T. Sjöstrand, S. Mrenna, P. Skands, PYTHIA 6.4 physics and manual, J. High Energy Phys. 05 (2006) 026, arXiv:hep-ph/0603175;
T. Sjöstrand, S. Mrenna, P. Skands, A brief introduction to PYTHIA 8.1, Comput. Phys. Commun. 178 (2008) 852, arXiv:0710.3820.
- [39] I. Belyaev, et al., Handling of the generation of primary events in GAUSS, the LHCb simulation framework, in: Nuclear Science Symposium Conference Record (NSS/MIC), IEEE, 2010, p. 1155.
- [40] D.J. Lange, The EVTGEN particle decay simulation package, Nucl. Instrum. Methods A 462 (2001) 152.
- [41] P. Golonka, Z. Was, PHOTOS Monte Carlo: a precision tool for QED corrections in Z and W decays, Eur. Phys. J. C 45 (2006) 97, arXiv:hep-ph/0506026.
- [42] Geant4 Collaboration, S. Agostinelli, et al., GEANT4: a simulation toolkit, Nucl. Instrum. Methods A 506 (2003) 250.
- [43] Geant4 Collaboration, J. Allison, et al., GEANT4 developments and applications, IEEE Trans. Nucl. Sci. 53 (2006) 270.
- [44] M. Clemencic, et al., The LHCb simulation application, GAUSS: design, evolution and experience, J. Phys. Conf. Ser. 331 (2011) 032023.
- [45] LHCb Collaboration, R. Aaij, et al., Observation of $B_s^0 \rightarrow \chi_{c1}\phi$ decay and study of $B^0 \rightarrow \chi_{c1,2}K^{*0}$ decays, Nucl. Phys. B 874 (2013) 663, arXiv:1305.6511.

- [46] LHCb Collaboration, R. Aaij, et al., Evidence for the decay $B \rightarrow J/\psi\omega$ and measurement of the relative branching fractions of B_s^0 meson decays to $J/\psi\eta$ and $J/\psi\eta'$, Nucl. Phys. B 867 (2013) 547, arXiv:1210.2631.
- [47] LHCb Collaboration, R. Aaij, et al., Observations of $B_s^0 \rightarrow \psi(2S)\eta$ and $B_{(s)}^0 \rightarrow \psi(2S)\pi^+\pi^-$ decays, Nucl. Phys. B 871 (2013) 403, arXiv:1302.6354.
- [48] F. Archilli, et al., Performance of the muon identification at LHCb, J. Instrum. 8 (2013) P10020, arXiv:1306.0249.
- [49] LHCb Collaboration, R. Aaij, et al., Measurement of the ratio of prompt χ_c to J/ψ production in pp collisions at $\sqrt{s} = 7$ TeV, Phys. Lett. B 718 (2012) 431, arXiv:1204.1462.
- [50] D. Savrina, Measurement of the branching fractions of the $B_s^0 \rightarrow J/\psi\eta$, $B_s^0 \rightarrow J/\psi\eta'$ and $B^0 \rightarrow J/\psi\omega^0$ decays in the LHCb experiment, PhD thesis, Institute for Theoretical and Experimental Physics, Moscow, 2013, CERN-THESIS-2013-229.
- [51] W.D. Hulsbergen, Decay chain fitting with a Kalman filter, Nucl. Instrum. Methods A 552 (2005) 566, arXiv: physics/0503191.
- [52] Particle Data Group, J. Beringer, et al., Review of particle physics, Phys. Rev. D 86 (2012) 010001, and 2013 partial update for the 2014 edition.
- [53] T. Skwarnicki, A study of the radiative cascade transitions between the Υ' and Υ resonances, PhD thesis, Institute of Nuclear Physics, Krakow, 1986, DESY-F31-86-02.
- [54] K.S. Cranmer, Kernel estimation in high-energy physics, Comput. Phys. Commun. 136 (2001) 198, arXiv:hep-ex/0011057.
- [55] LHCb Collaboration, R. Aaij, et al., Measurement of relative branching fractions of B decays to $\psi(2S)$ and J/ψ mesons, Eur. Phys. J. C 72 (2012) 2118, arXiv:1205.0918.

LHCb Collaboration

R. Aaij⁴¹, B. Adeva³⁷, M. Adinolfi⁴⁶, A. Affolder⁵², Z. Ajaltouni⁵,
 J. Albrecht⁹, F. Alessio³⁸, M. Alexander⁵¹, S. Ali⁴¹, G. Alkhazov³⁰,
 P. Alvarez Cartelle³⁷, A.A. Alves Jr^{25,38}, S. Amato², S. Amerio²²,
 Y. Amhis⁷, L. An³, L. Anderlini^{17,g}, J. Anderson⁴⁰, R. Andreassen⁵⁷,
 M. Andreotti^{16,f}, J.E. Andrews⁵⁸, R.B. Appleby⁵⁴,
 O. Aquines Gutierrez¹⁰, F. Archilli³⁸, A. Artamonov³⁵, M. Artuso⁵⁹,
 E. Aslanides⁶, G. Auriemma^{25,n}, M. Baalouch⁵, S. Bachmann¹¹,
 J.J. Back⁴⁸, A. Badalov³⁶, V. Balagura³¹, W. Baldini¹⁶, R.J. Barlow⁵⁴,
 C. Barschel³⁸, S. Barsuk⁷, W. Barter⁴⁷, V. Batozskaya²⁸, Th. Bauer⁴¹,
 A. Bay³⁹, J. Beddow⁵¹, F. Bedeschi²³, I. Bediaga¹, S. Belogurov³¹,
 K. Belous³⁵, I. Belyaev^{31,*}, E. Ben-Haim⁸, G. Bencivenni¹⁸,
 S. Benson⁵⁰, J. Benton⁴⁶, A. Berezhnoy³², R. Bernet⁴⁰, M.-O. Bettler⁴⁷,
 M. van Beuzekom⁴¹, A. Bien¹¹, S. Bifani⁴⁵, T. Bird⁵⁴, A. Bizzeti^{17,i},
 P.M. Bjørnstad⁵⁴, T. Blake⁴⁸, F. Blanc³⁹, J. Blouw¹⁰, S. Blusk⁵⁹,
 V. Bocci²⁵, A. Bondar³⁴, N. Bondar^{30,38}, W. Bonivento^{15,38}, S. Borghi⁵⁴,
 A. Borgia⁵⁹, M. Borsato⁷, T.J.V. Bowcock⁵², E. Bowen⁴⁰, C. Bozzi¹⁶,
 T. Brambach⁹, J. van den Brand⁴², J. Bressieux³⁹, D. Brett⁵⁴,
 M. Britsch¹⁰, T. Britton⁵⁹, N.H. Brook⁴⁶, H. Brown⁵², A. Bursche⁴⁰,
 G. Busetto^{22,g}, J. Buytaert³⁸, S. Cadeddu¹⁵, R. Calabrese^{16,f}, O. Callot⁷,
 M. Calvi^{20,k}, M. Calvo Gomez^{36,o}, A. Camboni³⁶, P. Campana^{18,38},
 D. Campora Perez³⁸, A. Carbone^{14,d}, G. Carboni^{24,l}, R. Cardinale^{19,38,j},
 A. Cardini¹⁵, H. Carranza-Mejia⁵⁰, L. Carson⁵⁰, K. Carvalho Akiba²,

- G. Casse ⁵², L. Cassina ²⁰, L. Castillo Garcia ³⁸, M. Cattaneo ³⁸,
 Ch. Cauet ⁹, R. Cenci ⁵⁸, M. Charles ⁸, Ph. Charpentier ³⁸, S.-F. Cheung ⁵⁵,
 N. Chiapolini ⁴⁰, M. Chrzaszcz ^{40,26}, K. Ciba ³⁸, X. Cid Vidal ³⁸,
 G. Ciezarek ⁵³, P.E.L. Clarke ⁵⁰, M. Clemencic ³⁸, H.V. Cliff ⁴⁷,
 J. Closier ³⁸, C. Coca ²⁹, V. Coco ³⁸, J. Cogan ⁶, E. Cogneras ⁵, P. Collins ³⁸,
 A. Comerma-Montells ¹¹, A. Contu ^{15,38}, A. Cook ⁴⁶, M. Coombes ⁴⁶,
 S. Coquereau ⁸, G. Corti ³⁸, M. Corvo ^{16,f}, I. Counts ⁵⁶, B. Couturier ³⁸,
 G.A. Cowan ⁵⁰, D.C. Craik ⁴⁸, M. Cruz Torres ⁶⁰, S. Cunliffe ⁵³,
 R. Currie ⁵⁰, C. D'Ambrosio ³⁸, J. Dalseno ⁴⁶, P. David ⁸, P.N.Y. David ⁴¹,
 A. Davis ⁵⁷, K. De Bruyn ⁴¹, S. De Capua ⁵⁴, M. De Cian ¹¹,
 J.M. De Miranda ¹, L. De Paula ², W. De Silva ⁵⁷, P. De Simone ¹⁸,
 D. Decamp ⁴, M. Deckenhoff ⁹, L. Del Buono ⁸, N. Déléage ⁴,
 D. Derkach ⁵⁵, O. Deschamps ⁵, F. Dettori ⁴², A. Di Canto ³⁸,
 H. Dijkstra ³⁸, S. Donleavy ⁵², F. Dordei ¹¹, M. Dorigo ³⁹,
 A. Dosil Suárez ³⁷, D. Dossett ⁴⁸, A. Dovbnya ⁴³, F. Dupertuis ³⁹,
 P. Durante ³⁸, R. Dzhelyadin ³⁵, A. Dziurda ²⁶, A. Dzyuba ³⁰, S. Easo ⁴⁹,
 U. Egede ⁵³, V. Egorychev ³¹, S. Eidelman ³⁴, S. Eisenhardt ⁵⁰,
 U. Eitschberger ⁹, R. Ekelhof ⁹, L. Eklund ^{51,38}, I. El Rifai ⁵,
 Ch. Elsasser ⁴⁰, S. Esen ¹¹, T. Evans ⁵⁵, A. Falabella ^{16,f}, C. Färber ¹¹,
 C. Farinelli ⁴¹, S. Farry ⁵², D. Ferguson ⁵⁰, V. Fernandez Albor ³⁷,
 F. Ferreira Rodrigues ¹, M. Ferro-Luzzi ³⁸, S. Filippov ³³, M. Fiore ^{16,f},
 M. Fiorini ^{16,f}, M. Firlej ²⁷, C. Fitzpatrick ³⁸, T. Fiutowski ²⁷,
 M. Fontana ¹⁰, F. Fontanelli ^{19,j}, R. Forty ³⁸, O. Francisco ², M. Frank ³⁸,
 C. Frei ³⁸, M. Frosini ^{17,38,g}, J. Fu ^{21,38}, E. Furfarò ^{24,l}, A. Gallas Torreira ³⁷,
 D. Galli ^{14,d}, S. Gallorini ²², S. Gambetta ^{19,j}, M. Gandelman ²,
 P. Gandini ⁵⁹, Y. Gao ³, J. Garofoli ⁵⁹, J. Garra Tico ⁴⁷, L. Garrido ³⁶,
 C. Gaspar ³⁸, R. Gauld ⁵⁵, L. Gavardi ⁹, E. Gersabeck ¹¹, M. Gersabeck ⁵⁴,
 T. Gershon ⁴⁸, Ph. Ghez ⁴, A. Gianelle ²², S. Giani' ³⁹, V. Gibson ⁴⁷,
 L. Giubega ²⁹, V.V. Gligorov ³⁸, C. Göbel ⁶⁰, D. Golubkov ³¹,
 A. Golutvin ^{53,31,38}, A. Gomes ^{1,a}, H. Gordon ³⁸, C. Gotti ²⁰,
 M. Grabalosa Gándara ⁵, R. Graciani Diaz ³⁶, L.A. Granado Cardoso ³⁸,
 E. Graugés ³⁶, G. Graziani ¹⁷, A. Grecu ²⁹, E. Greening ⁵⁵, S. Gregson ⁴⁷,
 P. Griffith ⁴⁵, L. Grillo ¹¹, O. Grünberg ⁶², B. Gui ⁵⁹, E. Gushchin ³³,
 Yu. Guz ^{35,38}, T. Gys ³⁸, C. Hadjivasilou ⁵⁹, G. Haefeli ³⁹, C. Haen ³⁸,
 S.C. Haines ⁴⁷, S. Hall ⁵³, B. Hamilton ⁵⁸, T. Hampson ⁴⁶, X. Han ¹¹,
 S. Hansmann-Menzemer ¹¹, N. Harnew ⁵⁵, S.T. Harnew ⁴⁶, J. Harrison ⁵⁴,
 T. Hartmann ⁶², J. He ³⁸, T. Head ³⁸, V. Heijne ⁴¹, K. Hennessy ⁵²,

- P. Henrard ⁵, L. Henry ⁸, J.A. Hernando Morata ³⁷, E. van Herwijnen ³⁸,
 M. Heß ⁶², A. Hicheur ¹, D. Hill ⁵⁵, M. Hoballah ⁵, C. Hombach ⁵⁴,
 W. Hulsbergen ⁴¹, P. Hunt ⁵⁵, N. Hussain ⁵⁵, D. Hutchcroft ⁵², D. Hynds ⁵¹,
 M. Idzik ²⁷, P. Ilten ⁵⁶, R. Jacobsson ³⁸, A. Jaeger ¹¹, J. Jalocha ⁵⁵,
 E. Jans ⁴¹, P. Jaton ³⁹, A. Jawahery ⁵⁸, M. Jezabek ²⁶, F. Jing ³, M. John ⁵⁵,
 D. Johnson ⁵⁵, C.R. Jones ⁴⁷, C. Joram ³⁸, B. Jost ³⁸, N. Jurik ⁵⁹,
 M. Kaballo ⁹, S. Kandybei ⁴³, W. Kanso ⁶, M. Karacson ³⁸,
 T.M. Karbach ³⁸, M. Kelsey ⁵⁹, I.R. Kenyon ⁴⁵, T. Ketel ⁴², B. Khanji ²⁰,
 C. Khurewathanakul ³⁹, S. Klaver ⁵⁴, O. Kochebina ⁷, M. Kolpin ¹¹,
 I. Komarov ³⁹, R.F. Koopman ⁴², P. Koppenburg ^{41,38}, M. Korolev ³²,
 A. Kozlinskiy ⁴¹, L. Kravchuk ³³, K. Kreplin ¹¹, M. Kreps ⁴⁸, G. Krocker ¹¹,
 P. Krokovny ³⁴, F. Kruse ⁹, M. Kucharczyk ^{20,26,38,k}, V. Kudryavtsev ³⁴,
 K. Kurek ²⁸, T. Kvaratskheliya ³¹, V.N. La Thi ³⁹, D. Lacarrere ³⁸,
 G. Lafferty ⁵⁴, A. Lai ¹⁵, D. Lambert ⁵⁰, R.W. Lambert ⁴², E. Lanciotti ³⁸,
 G. Lanfranchi ¹⁸, C. Langenbruch ³⁸, B. Langhans ³⁸, T. Latham ⁴⁸,
 C. Lazzeroni ⁴⁵, R. Le Gac ⁶, J. van Leerdam ⁴¹, J.-P. Lees ⁴, R. Lefèvre ⁵,
 A. Leflat ³², J. Lefrançois ⁷, S. Leo ²³, O. Leroy ⁶, T. Lesiak ²⁶,
 B. Leverington ¹¹, Y. Li ³, M. Liles ⁵², R. Lindner ³⁸, C. Linn ³⁸,
 F. Lionetto ⁴⁰, B. Liu ¹⁵, G. Liu ³⁸, S. Lohn ³⁸, I. Longstaff ⁵¹, J.H. Lopes ²,
 N. Lopez-March ³⁹, P. Lowdon ⁴⁰, H. Lu ³, D. Lucchesi ^{22,q}, H. Luo ⁵⁰,
 A. Lupato ²², E. Luppi ^{16,f}, O. Lupton ⁵⁵, F. Machefert ⁷,
 I.V. Machikhiliyan ³¹, F. Maciuc ²⁹, O. Maev ³⁰, S. Malde ⁵⁵, G. Manca ^{15,e},
 G. Mancinelli ⁶, M. Manzali ^{16,f}, J. Maratas ⁵, J.F. Marchand ⁴,
 U. Marconi ¹⁴, C. Marin Benito ³⁶, P. Marino ^{23,s}, R. Märki ³⁹, J. Marks ¹¹,
 G. Martellotti ²⁵, A. Martens ⁸, A. Martín Sánchez ⁷, M. Martinelli ⁴¹,
 D. Martinez Santos ⁴², F. Martinez Vidal ⁶⁴, D. Martins Tostes ²,
 A. Massafferri ¹, R. Matev ³⁸, Z. Mathe ³⁸, C. Matteuzzi ²⁰,
 A. Mazurov ^{16,f}, M. McCann ⁵³, J. McCarthy ⁴⁵, A. McNab ⁵⁴,
 R. McNulty ¹², B. McSkelly ⁵², B. Meadows ^{57,55}, F. Meier ⁹,
 M. Meissner ¹¹, M. Merk ⁴¹, D.A. Milanes ⁸, M.-N. Minard ⁴,
 J. Molina Rodriguez ⁶⁰, S. Monteil ⁵, D. Moran ⁵⁴, M. Morandin ²²,
 P. Morawski ²⁶, A. Mordà ⁶, M.J. Morello ^{23,s}, J. Moron ²⁷, R. Mountain ⁵⁹,
 F. Muheim ⁵⁰, K. Müller ⁴⁰, R. Muresan ²⁹, B. Muster ³⁹, P. Naik ⁴⁶,
 T. Nakada ³⁹, R. Nandakumar ⁴⁹, I. Nasteva ², M. Needham ⁵⁰, N. Neri ²¹,
 S. Neubert ³⁸, N. Neufeld ³⁸, M. Neuner ¹¹, A.D. Nguyen ³⁹,
 T.D. Nguyen ³⁹, C. Nguyen-Mau ^{39,p}, M. Nicol ⁷, V. Niess ⁵, R. Niet ⁹,
 N. Nikitin ³², T. Nikodem ¹¹, A. Novoselov ³⁵, A. Oblakowska-Mucha ²⁷,

- V. Obraztsov ³⁵, S. Oggero ⁴¹, S. Ogilvy ⁵¹, O. Okhrimenko ⁴⁴,
 R. Oldeman ^{15,e}, G. Onderwater ⁶⁵, M. Orlandea ²⁹,
 J.M. Otalora Goicochea ², P. Owen ⁵³, A. Oyanguren ⁶⁴, B.K. Pal ⁵⁹,
 A. Palano ^{13,c}, F. Palombo ^{21,t}, M. Palutan ¹⁸, J. Panman ³⁸,
 A. Papanestis ^{49,38}, M. Pappagallo ⁵¹, C. Parkes ⁵⁴, C.J. Parkinson ⁹,
 G. Passaleva ¹⁷, G.D. Patel ⁵², M. Patel ⁵³, C. Patrignani ^{19,j},
 A. Pazos Alvarez ³⁷, A. Pearce ⁵⁴, A. Pellegrino ⁴¹, M. Pepe Altarelli ³⁸,
 S. Perazzini ^{14,d}, E. Perez Trigo ³⁷, P. Perret ⁵, M. Perrin-Terrin ⁶,
 L. Pescatore ⁴⁵, E. Pesen ⁶⁶, K. Petridis ⁵³, A. Petrolini ^{19,j},
 E. Picatoste Olloqui ³⁶, B. Pietrzyk ⁴, T. Pilai ⁴⁸, D. Pinci ²⁵, A. Pistone ¹⁹,
 S. Playfer ⁵⁰, M. Plo Casasus ³⁷, F. Polci ⁸, A. Poluektov ^{48,34},
 I. Polyakov ³¹, E. Polycarpo ², A. Popov ³⁵, D. Popov ¹⁰, B. Popovici ²⁹,
 C. Potterat ², A. Powell ⁵⁵, J. Prisciandaro ³⁹, A. Pritchard ⁵², C. Prouve ⁴⁶,
 V. Pugatch ⁴⁴, A. Puig Navarro ³⁹, G. Punzi ^{23,r}, W. Qian ⁴, B. Rachwal ²⁶,
 J.H. Rademacker ⁴⁶, B. Rakotomiaramanana ³⁹, M. Rama ¹⁸,
 M.S. Rangel ², I. Raniuk ⁴³, N. Rauschmayr ³⁸, G. Raven ⁴², S. Reichert ⁵⁴,
 M.M. Reid ⁴⁸, A.C. dos Reis ¹, S. Ricciardi ⁴⁹, A. Richards ⁵³,
 K. Rinnert ⁵², V. Rives Molina ³⁶, D.A. Roa Romero ⁵, P. Robbe ⁷,
 A.B. Rodrigues ¹, E. Rodrigues ⁵⁴, P. Rodriguez Perez ⁵⁴, S. Roiser ³⁸,
 V. Romanovsky ³⁵, A. Romero Vidal ³⁷, M. Rotondo ²², J. Rouvinet ³⁹,
 T. Ruf ³⁸, F. Ruffini ²³, H. Ruiz ³⁶, P. Ruiz Valls ⁶⁴, G. Sabatino ^{25,l},
 J.J. Saborido Silva ³⁷, N. Sagidova ³⁰, P. Sail ⁵¹, B. Saitta ^{15,e},
 V. Salustino Guimaraes ², C. Sanchez Mayordomo ⁶⁴,
 B. Sanmartin Sedes ³⁷, R. Santacesaria ²⁵, C. Santamarina Rios ³⁷,
 E. Santovetti ^{24,l}, M. Sapunov ⁶, A. Sarti ^{18,m}, C. Satriano ^{25,n}, A. Satta ²⁴,
 M. Savrie ^{16,f}, D. Savrina ^{31,32}, M. Schiller ⁴², H. Schindler ³⁸,
 M. Schlupp ⁹, M. Schmelling ¹⁰, B. Schmidt ³⁸, O. Schneider ³⁹,
 A. Schopper ³⁸, M.-H. Schune ⁷, R. Schwemmer ³⁸, B. Sciascia ¹⁸,
 A. Sciubba ²⁵, M. Seco ³⁷, A. Semennikov ³¹, K. Senderowska ²⁷,
 I. Sepp ⁵³, N. Serra ⁴⁰, J. Serrano ⁶, L. Sestini ²², P. Seyfert ¹¹,
 M. Shapkin ³⁵, I. Shapoval ^{16,43,f}, Y. Shcheglov ³⁰, T. Shears ⁵²,
 L. Shekhtman ³⁴, V. Shevchenko ⁶³, A. Shires ⁹, R. Silva Coutinho ⁴⁸,
 G. Simi ²², M. Sirendi ⁴⁷, N. Skidmore ⁴⁶, T. Skwarnicki ⁵⁹, N.A. Smith ⁵²,
 E. Smith ^{55,49}, E. Smith ⁵³, J. Smith ⁴⁷, M. Smith ⁵⁴, H. Snoek ⁴¹,
 M.D. Sokoloff ⁵⁷, F.J.P. Soler ⁵¹, F. Soomro ³⁹, D. Souza ⁴⁶,
 B. Souza De Paula ², B. Spaan ⁹, A. Sparkes ⁵⁰, F. Spinella ²³,
 P. Spradlin ⁵¹, F. Stagni ³⁸, S. Stahl ¹¹, O. Steinkamp ⁴⁰, O. Stenyakin ³⁵,

S. Stevenson ⁵⁵, S. Stoica ²⁹, S. Stone ⁵⁹, B. Storaci ⁴⁰, S. Stracka ^{23,38},
 M. Stratificiuc ²⁹, U. Straumann ⁴⁰, R. Stroili ²², V.K. Subbiah ³⁸, L. Sun ⁵⁷,
 W. Sutcliffe ⁵³, K. Swientek ²⁷, S. Swientek ⁹, V. Syropoulos ⁴²,
 M. Szczechowski ²⁸, P. Szczypka ^{39,38}, D. Szilard ², T. Szumlak ²⁷,
 S. T'Jampens ⁴, M. Teklishyn ⁷, G. Tellarini ^{16,f}, E. Teodorescu ²⁹,
 F. Teubert ³⁸, C. Thomas ⁵⁵, E. Thomas ³⁸, J. van Tilburg ⁴¹, V. Tisserand ⁴,
 M. Tobin ³⁹, S. Tolk ⁴², L. Tomassetti ^{16,f}, D. Tonelli ³⁸,
 S. Topp-Joergensen ⁵⁵, N. Torr ⁵⁵, E. Tournefier ⁴, S. Tourneur ³⁹,
 M.T. Tran ³⁹, M. Tresch ⁴⁰, A. Tsaregorodtsev ⁶, P. Tsopelas ⁴¹,
 N. Tuning ⁴¹, M. Ubeda Garcia ³⁸, A. Ukleja ²⁸, A. Ustyuzhanin ⁶³,
 U. Uwer ¹¹, V. Vagnoni ¹⁴, G. Valenti ¹⁴, A. Vallier ⁷, R. Vazquez Gomez ¹⁸,
 P. Vazquez Regueiro ³⁷, C. Vázquez Sierra ³⁷, S. Vecchi ¹⁶, J.J. Velthuis ⁴⁶,
 M. Veltri ^{17,h}, G. Veneziano ³⁹, M. Vesterinen ¹¹, B. Viaud ⁷, D. Vieira ²,
 M. Vieites Diaz ³⁷, X. Vilasis-Cardona ^{36,o}, A. Vollhardt ⁴⁰,
 D. Volyanskyy ¹⁰, D. Voong ⁴⁶, A. Vorobyev ³⁰, V. Vorobyev ³⁴, C. Voß ⁶²,
 H. Voss ¹⁰, J.A. de Vries ⁴¹, R. Waldi ⁶², C. Wallace ⁴⁸, R. Wallace ¹²,
 J. Walsh ²³, S. Wandernoth ¹¹, J. Wang ⁵⁹, D.R. Ward ⁴⁷, N.K. Watson ⁴⁵,
 A.D. Webber ⁵⁴, D. Websdale ⁵³, M. Whitehead ⁴⁸, J. Wicht ³⁸,
 D. Wiedner ¹¹, G. Wilkinson ⁵⁵, M.P. Williams ⁴⁵, M. Williams ⁵⁶,
 F.F. Wilson ⁴⁹, J. Wimberley ⁵⁸, J. Wishahi ⁹, W. Wislicki ²⁸, M. Witek ²⁶,
 G. Wormser ⁷, S.A. Wotton ⁴⁷, S. Wright ⁴⁷, S. Wu ³, K. Wyllie ³⁸,
 Y. Xie ⁶¹, Z. Xing ⁵⁹, Z. Xu ³⁹, Z. Yang ³, X. Yuan ³, O. Yushchenko ³⁵,
 M. Zangoli ¹⁴, M. Zavertyaev ^{10,b}, F. Zhang ³, L. Zhang ⁵⁹, W.C. Zhang ¹²,
 Y. Zhang ³, A. Zhelezov ¹¹, A. Zhokhov ³¹, L. Zhong ³, A. Zvyagin ³⁸

¹ Centro Brasileiro de Pesquisas Físicas (CBPF), Rio de Janeiro, Brazil² Universidade Federal do Rio de Janeiro (UFRJ), Rio de Janeiro, Brazil³ Center for High Energy Physics, Tsinghua University, Beijing, China⁴ LAPP, Université de Savoie, CNRS/IN2P3, Annecy-Le-Vieux, France⁵ Clermont Université, Université Blaise Pascal, CNRS/IN2P3, LPC, Clermont-Ferrand, France⁶ CPPM, Aix-Marseille Université, CNRS/IN2P3, Marseille, France⁷ LAL, Université Paris-Sud, CNRS/IN2P3, Orsay, France⁸ LPNHE, Université Pierre et Marie Curie, Université Paris Diderot, CNRS/IN2P3, Paris, France⁹ Fakultät Physik, Technische Universität Dortmund, Dortmund, Germany¹⁰ Max-Planck-Institut für Kernphysik (MPIK), Heidelberg, Germany¹¹ Physikalisches Institut, Ruprecht-Karls-Universität Heidelberg, Heidelberg, Germany¹² School of Physics, University College Dublin, Dublin, Ireland¹³ Sezione INFN di Bari, Bari, Italy¹⁴ Sezione INFN di Bologna, Bologna, Italy¹⁵ Sezione INFN di Cagliari, Cagliari, Italy¹⁶ Sezione INFN di Ferrara, Ferrara, Italy¹⁷ Sezione INFN di Firenze, Firenze, Italy¹⁸ Laboratori Nazionali dell'INFN di Frascati, Frascati, Italy¹⁹ Sezione INFN di Genova, Genova, Italy

- ²⁰ Sezione INFN di Milano Bicocca, Milano, Italy
²¹ Sezione INFN di Milano, Milano, Italy
²² Sezione INFN di Padova, Padova, Italy
²³ Sezione INFN di Pisa, Pisa, Italy
²⁴ Sezione INFN di Roma Tor Vergata, Roma, Italy
²⁵ Sezione INFN di Roma La Sapienza, Roma, Italy
²⁶ Henryk Niewodniczanski Institute of Nuclear Physics, Polish Academy of Sciences, Kraków, Poland
²⁷ AGH – University of Science and Technology, Faculty of Physics and Applied Computer Science, Kraków, Poland
²⁸ National Center for Nuclear Research (NCBJ), Warsaw, Poland
²⁹ Horia Hulubei National Institute of Physics and Nuclear Engineering, Bucharest-Magurele, Romania
³⁰ Petersburg Nuclear Physics Institute (PNPI), Gatchina, Russia
³¹ Institute of Theoretical and Experimental Physics (ITEP), Moscow, Russia
³² Institute of Nuclear Physics, Moscow State University (SINP MSU), Moscow, Russia
³³ Institute for Nuclear Research of the Russian Academy of Sciences (INR RAN), Moscow, Russia
³⁴ Budker Institute of Nuclear Physics (SB RAS) and Novosibirsk State University, Novosibirsk, Russia
³⁵ Institute for High Energy Physics (IHEP), Protvino, Russia
³⁶ Universitat de Barcelona, Barcelona, Spain
³⁷ Universidad de Santiago de Compostela, Santiago de Compostela, Spain
³⁸ European Organization for Nuclear Research (CERN), Geneva, Switzerland
³⁹ Ecole Polytechnique Fédérale de Lausanne (EPFL), Lausanne, Switzerland
⁴⁰ Physik-Institut, Universität Zürich, Zürich, Switzerland
⁴¹ Nikhef National Institute for Subatomic Physics, Amsterdam, The Netherlands
⁴² Nikhef National Institute for Subatomic Physics and VU University Amsterdam, Amsterdam, The Netherlands
⁴³ NSC Kharkiv Institute of Physics and Technology (NSC KIPT), Kharkiv, Ukraine
⁴⁴ Institute for Nuclear Research of the National Academy of Sciences (KINR), Kyiv, Ukraine
⁴⁵ University of Birmingham, Birmingham, United Kingdom
⁴⁶ H.H. Wills Physics Laboratory, University of Bristol, Bristol, United Kingdom
⁴⁷ Cavendish Laboratory, University of Cambridge, Cambridge, United Kingdom
⁴⁸ Department of Physics, University of Warwick, Coventry, United Kingdom
⁴⁹ STFC Rutherford Appleton Laboratory, Didcot, United Kingdom
⁵⁰ School of Physics and Astronomy, University of Edinburgh, Edinburgh, United Kingdom
⁵¹ School of Physics and Astronomy, University of Glasgow, Glasgow, United Kingdom
⁵² Oliver Lodge Laboratory, University of Liverpool, Liverpool, United Kingdom
⁵³ Imperial College London, London, United Kingdom
⁵⁴ School of Physics and Astronomy, University of Manchester, Manchester, United Kingdom
⁵⁵ Department of Physics, University of Oxford, Oxford, United Kingdom
⁵⁶ Massachusetts Institute of Technology, Cambridge, MA, United States
⁵⁷ University of Cincinnati, Cincinnati, OH, United States
⁵⁸ University of Maryland, College Park, MD, United States
⁵⁹ Syracuse University, Syracuse, NY, United States
⁶⁰ Pontifícia Universidade Católica do Rio de Janeiro (PUC-Rio), Rio de Janeiro, Brazil ^u
⁶¹ Institute of Particle Physics, Central China Normal University, Wuhan, Hubei, China ^v
⁶² Institut für Physik, Universität Rostock, Rostock, Germany ^w
⁶³ National Research Centre Kurchatov Institute, Moscow, Russia ^x
⁶⁴ Instituto de Fisica Corpuscular (IFIC), Universitat de Valencia-CSIC, Valencia, Spain ^y
⁶⁵ KVI – University of Groningen, Groningen, The Netherlands ^z
⁶⁶ Celal Bayar University, Manisa, Turkey ^{aa}

^{*} Corresponding author.E-mail address: Ivan.Belyaev@itep.ru (I. Belyaev).^a Universidade Federal do Triângulo Mineiro (UFTM), Uberaba-MG, Brazil.^b P.N. Lebedev Physical Institute, Russian Academy of Science (LPI RAS), Moscow, Russia.^c Università di Bari, Bari, Italy.^d Università di Bologna, Bologna, Italy.^e Università di Cagliari, Cagliari, Italy.

f Università di Ferrara, Ferrara, Italy.

g Università di Firenze, Firenze, Italy.

h Università di Urbino, Urbino, Italy.

i Università di Modena e Reggio Emilia, Modena, Italy.

j Università di Genova, Genova, Italy.

k Università di Milano Bicocca, Milano, Italy.

l Università di Roma Tor Vergata, Roma, Italy.

m Università di Roma La Sapienza, Roma, Italy.

n Università della Basilicata, Potenza, Italy.

o LIFAELS, La Salle, Universitat Ramon Llull, Barcelona, Spain.

p Hanoi University of Science, Hanoi, Viet Nam.

q Università di Padova, Padova, Italy.

r Università di Pisa, Pisa, Italy.

s Scuola Normale Superiore, Pisa, Italy.

t Università degli Studi di Milano, Milano, Italy.

u Associated to Universidade Federal do Rio de Janeiro (UFRJ), Rio de Janeiro, Brazil.

v Associated to Center for High Energy Physics, Tsinghua University, Beijing, China.

w Associated to Physikalisches Institut, Ruprecht-Karls-Universität Heidelberg, Heidelberg, Germany.

x Associated to Institute of Theoretical and Experimental Physics (ITEP), Moscow, Russia.

y Associated to Universitat de Barcelona, Barcelona, Spain.

z Associated to Nikhef National Institute for Subatomic Physics, Amsterdam, The Netherlands.

aa Associated to European Organization for Nuclear Research (CERN), Geneva, Switzerland.